Proc. Indian Acad. Sci. (Earth Planet. Sci.), Vol. 104, No. 1, March 1995, pp. 115–129.

A simulation of upper crustal stresses for great and moderate thrust earthquakes of the Himalaya

R CHANDER and V K GAHALAUT
Department of Earth Sciences, University of Roorkee, Roorkee 247 667, India

MS received 13 February 1995; revised 7 April 1995

Abstract. We assume that great and moderate Himalayan earthquakes occur through reactivation of subhorizontal thrust faults by frictional failure under the action of stresses induced by Himalayan topography, isostasy related buoyancy forces, crustal overburden and plate tectonic causes. Estimates of stresses are based on two dimensional plane strain calculations using analytical formulae of elasticity theory and rock mechanics under suitable simplifying assumptions. Considerable attention is focussed on a point on the detachment at a depth of 17 km below mean sea level under the surface trace of the Main Central Thrust (MCT). According to recent views, great Himalayan earthquakes should nucleate in the detachment in the vicinity of such a point. Also many moderate earthquakes occur on the detachment similarly under the MCT. Vertical and horizontal normal stresses of 622 and 262 MPa and a corresponding shear stress of 26 MPa are estimated for this point due to topography, buoyancy and overburden. For fault friction coefficient varying between 0·3 to 1·0, estimates of plate tectonic stress required are in the range of 386 to 434 MPa, when the cumulative principal stresses are oriented favourably for reactivation of the detachment. Estimates of shear stress mobilized at the same point would be from 27 to 32 MPa for the identical range of fault friction coefficient. Our calculations suggest that presence of pore water in the fault zones is essential for reactivation. Pore pressure required is between 535 to 595 MPa for friction coefficient in the range of 0·3 to 1·0 and it is less than lithostatic stress of 603 MPa at the above point. For the specific nominal value of 0·65 for fault friction coefficient, the estimated values of plate tectonic stress, shear stress and pore pressure at the above point on the detachment are 410 MPa, 30 MPa and 580 MPa respectively. Similar estimates are obtained also for shallower points on the detachment up to the southern limit of the Outer Himalaya. Our estimates of the plate tectonic stress, shear stress and pore pressure for reactivation of upper crustal thrust faults compare favourably with those quoted in the literature.

Keywords. Crustal stresses; earthquakes; pore pressure; Himalaya.

1. Introduction

Differential relative uplift between the Higher, Lesser and Outer Himalaya and the occurrence of earthquakes are manifestations of relentless deformation and stress accumulation in the Himalayan upper crust due to the convergence of Indian and Eurasian lithospheric plates. Thus simulation of the upper crustal stress field in the Himalaya is of considerable importance as, potentially, it could provide valuable constraints for geodynamic models of the region including models of source processes for great and moderate Himalayan earthquakes. The latter objective is of main interest to us in this article.

The specific stress simulation problem attempted is identified from a review of recent literature on great and moderate Himalayan earthquakes. Several recent studies (Seeber and Armbruster 1981; Baranowski *et al* 1984; Ni and Barazangi 1984; Chander 1988,

1989; Molnar 1990; Gahalaut and Chander 1992; Yeats and Lillie 1991 and Gahalaut *et al* 1994) on great Himalayan earthquakes (figure 1a) suggest persuasively that they occur by extended ruptures in low angle intra-crustal thrust faults. According to some investigators (e.g. Molnar 1990) atleast three of the four great Himalayan earthquakes of the past 100 years occurred on down dip extension of the listric Main Boundary Thrust (MBT) whose surface outcrop demarcates the conventional boundary between the Outer and Lesser Himalaya (Gansser 1964).On the other hand, Seeber and Armbruster (1981) have argued that all four great earthquakes occurred on the detachment (figure 1b), a low angle thrust fault type boundary surface between the underthrusting Indian shield material and the overlying Himalayan rocks. Simulations by Chander (1988), Gahalaut and Chander (1992) and Gahalaut *et al* (1994) suggest that the causative ruptures of these earthquakes may extend in the detachment upto a depth of about 17 km below mean sea level (MSL). This limit should lie geographically beneath the surface trace of Main Central Thrust (MCT), the conventional boundary between the Lesser and Higher Himalaya (Gansser 1964). On the other hand, studies related to moderate Himalayan earthquakes (e.g., Baranowski *et al* 1984; Ni and Barazangi 1984; Molnar 1990 and Zhao and Helmberger 1991) suggest that they have focal depths of 10 to 18 km and occur either on the detachment itself or on low angle thrust faults near the detachment (figure 1b). Based on the available fault plane solution data (Fitch 1970; Baranowski *et al* 1984; Ni and Barazangi 1984 and Molnar 1990) for dips of the faults responsible for these moderate earthquakes (figure 1a and b) as well as the dip of the detachment (Seeber and Armbruster 1981; Ni and Barazangi 1984; Chander 1988, 1989; Molnar 1990; Gahalaut and Chander 1992; Zhao *et al* 1993), we make the simplifying assumption for our calculations that all great and moderate Himalayan earthquakes occur on thrust faults having the same gentle dip and consider a nominal value 5° for it. For the sake of brevity, generality and rigour in the following discussion, we refer to these earthquake generating faults including the detachment as subhorizontal thrust faults. We adopt

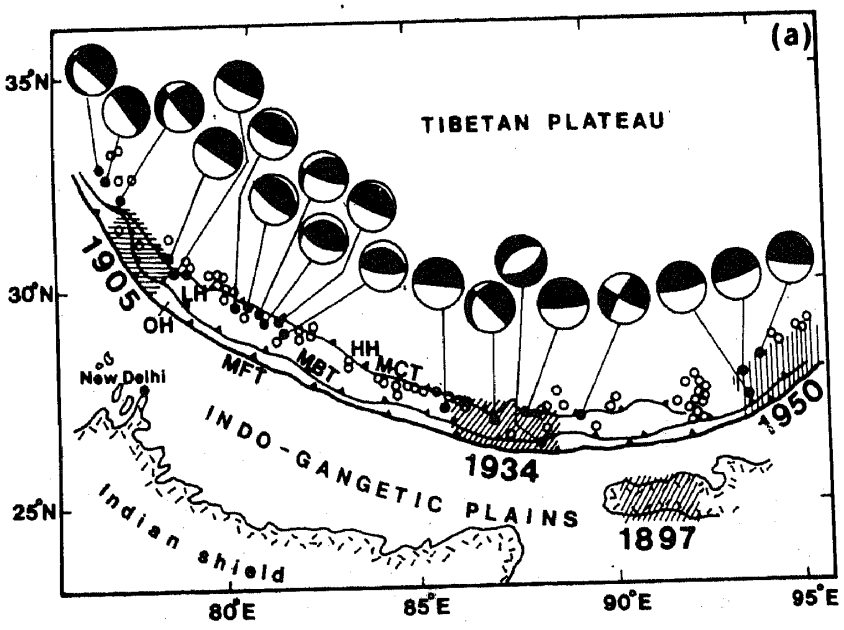

Figure 1a. (*Continued*)

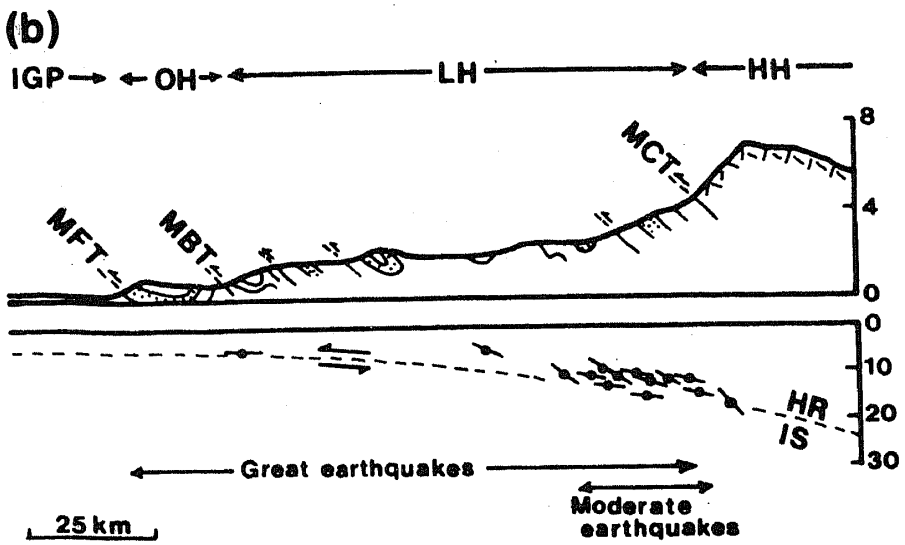

Figures 1a & b. Figures 1(a) and (b) provide a summary of our present knowledge about the distribution of great and moderate Himalayan earthquakes. In figure 1(a) the shaded areas identified with the dates of 1897, 1905, 1934 and 1950 indicate the inferred rupture zones of the four great Himalayan earthquakes of the last 100 years. Epicentres of moderate Himalayan earthquakes of the past 30 years are shown by small open circles. Fault plane solutions of 19 such earthquakes (epicentres shown by solid circles) based on waveform synthesis have been reported so far and are displayed by the beachballs. The background geology is after Gansser (1964). The abbreviations are as follows. MFT- Main Frontal Thrust; MBT- Main Boundary Thrust; MCT- Main Central Thrust; OH- Outer Himalaya; LH- Lesser Himalaya and HH- Higher Himalaya. **Figure 1(b)** which is again in two parts, presents a generalized cross section of the Himalayan crust when viewed normal to the strike of the Himalaya. The upper part shows the Himalayan surface topography and geology in a schematic manner. The lower part shows by dots the foci of several moderate earthquakes projected onto the plane of the section (see Ni and Barazangi 1984). The short line through each dot represents schematically the caustive fault inferred by selecting one of the nodal planes of the respective fault plane solution as the fault plane. The dashed line marks the boundary between Himalayan (HR) and Indian shield (IS) rocks. It constitutes the detachment surface of Seeber and Armbruster (1981). The width of the detachment ruptured during a great Himalayan earthquake typically is indicated. IGP stands for Indo-Gangetic plains.

the model that earthquakes occur by reactivation of these faults through frictional failure and seek estimates of stresses that could lead to such failure.

Our procedure for estimating earthquake generating stresses under the Outer and Lesser Himalaya is as follows. At an upper crustal point of interest, we first estimate approximately the stresses due to Himalayan topography, isostasy related buoyancy forces and the crustal overburden using approximate but relatively simple analytical formulas of elasticity theory. We then try to estimate the resultant plate tectonic stress that when added to these stresses would lead to failure on the sub-horizontal thrust faults in accord with the Coulomb-Mohr criterion of frictional failure. This procedure of estimating plate tectonic stresses, although conceived independently, is comparable to that adopted by Sonder (see Zoback 1992) for estimation of regional crustal stresses starting from estimates about superimposed local stress fields of tectonic origin.

2. Theory

2.1 *Simulation of stresses due to topographic load*

We approximate the topography of the Himalaya and Tibet as a combination of (i) a linearly increasing load simulating the topography of the Outer and Lesser Himalaya, (ii) a sequence of stepwise varying loads simulating grossly the topography of the Higher and Tethys Himalaya and (iii) a constant load simulating the Tibetan plateau (figure 2). Such a model was used also by Burchfiel and Royden (1985) in their simulation of normal faults in the Higher Himalaya. We assume that Boussinesq's (Jaeger and Cook 1969, p. 274–276) expressions for stresses due to a line load on the surface of an elastic half space may be used as Green's function kernels to compute through convolution the stresses generated by such a general topography. The density of the topographic material is assumed to be 2800 kg m^{-3}.

2.2 *Simulation of stresses due to buoyancy forces*

We adopt the crustal thickness model proposed for the Himalaya by Lyon-Caen and Molnar (1985) for estimation of buoyancy forces. They inferred the depth of crustmantle boundary under the Himalaya (figure 2) from an analysis of gravity data. We assume that the magnitude of the buoyancy force in response to the isostatic compensation of the Himalayan and Tibetan topography is a function of the crustal thickness in excess of 40 km. A density contrast of 400 kg m^{-3} between the crustal and mantle materials is assumed

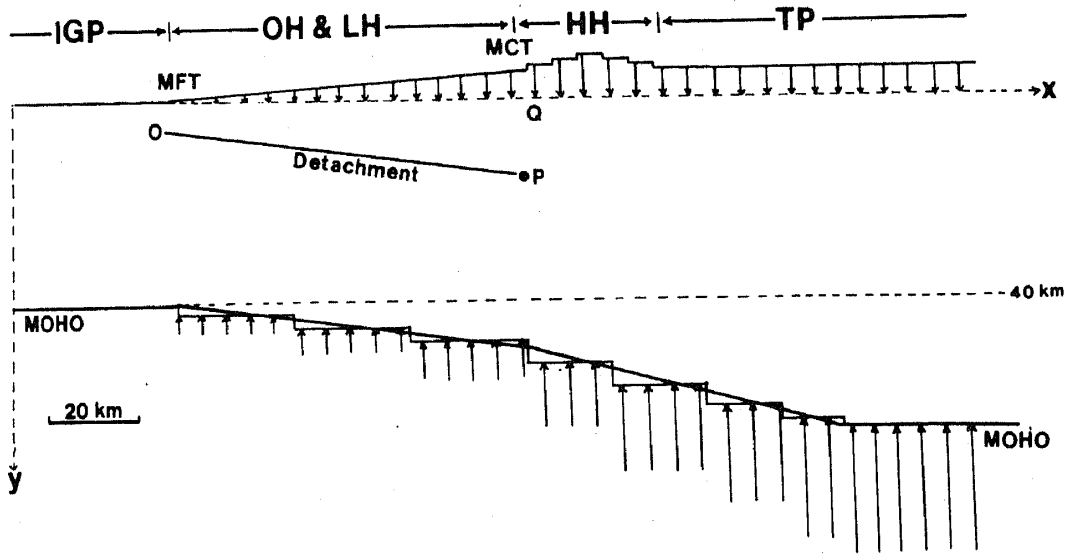

Figure 2. Idealized cross section of the Himalayan crust normal to the strike of the Himalaya. The figure is partly comparable to figure 1 (b). The major additions in the present figure are that topography of the Tibetan plateau (TP) as well as the moho are shown schematically. The major difference is that the Himalayan topography is even more generalized for computational purposes. The section of the detachment involved in great earthquakes is also shown in cross section by the straight line. The arrows pointing downward indicate schematically the topographic load and those pointing upward, the isostasy related buoyancy load (see text). This figure also serves as an index in that calculations for point P are shown in figure 4(a) and (b), for the section OP of the detachment in figure 5 and for the hypothetical vertical line PQ in figure 6.

to determine the magnitude of buoyancy loads. We approximate the form of crust-mantle boundary given by Lyon-Caen and Molnar (1985) as a series of steps of increasing depth as we proceed across the Himalaya towards Tibet (figure 2). Thus the buoyancy force acts vertically upward in our simulation. The stresses in the upper crust arising from them are estimated approximately by again using the above mentioned Boussinesq's formulas.

We are aware of the discussion in the literature as to whether the Himalaya are fully compensated isostatically (e.g., Karner and Watts 1983 and Lyon-Caen and Molnar 1985). However, we have assumed full compensation for our calculations.

2.3 *Simulation of stresses due to crustal overburden*

The term crustal overburden as used by us means the mass of rock between the MSL and the point of interest in the crust. To calculate the stresses due to it we adopt the elastic, Poisson solid, half-space model in which the vertical normal stress is the weight per unit area of the overburden and the horizontal normal stress is one third of the vertical normal stress (Jaeger and Cook 1969). Again a density of 2800 kg m^{-3} is assumed.

2.4 *Simulation of horizontal compressive stresses of plate tectonic origin*

We can now estimate the plate tectonic stress which when superimposed on the above stresses pointwise in the crust would promote frictional failure on the subhorizontal thrust faults. As discussed by many authors (e.g., Forsyth and Uyeda 1975 and Bott and Kusznir 1984) there may be several causes for plate tectonic stresses at a given point in the earth's crust. But through our calculations we are able to estimate only the resultant of these stresses at each crustal point.

We assume that the plate tectonic stress at each crustal point would be compressive, horizontal and normal to the local strike of the Himalaya. Thus we have to estimate σ_{xP} in the notation given in the Appendix. The expression available for the purpose is the following form of the Coulomb-Mohr criterion for frictional failure on crustal faults.

$$\tau_F = (\sigma_F - \mathrm{p}) \tan \phi \tag{1}$$

τ_F and σ_F are given through the expressions (e.g. see Jaeger and Cook 1969)

$$\tau_F = 0{\cdot}5(\sigma_{xP} + \sigma_{xc} - \sigma_{yc}) \sin 2\delta + \tau_{xyc} \cos 2\delta \tag{2}$$

$$\sigma_F = (\sigma_{xP} + \sigma_{xc}) \sin^2 \delta + \sigma_{yc} \cos^2 \delta + \tau_{xyc} \sin 2\delta. \tag{3}$$

It follows from an application of Mohr circle theory to the present problem that the magnitude of σ_{xP} is a single valued function of θ_R, the angle between the resultant maximum principal stress σ_{1R} due to the combined effect of topography, buoyancy, crustal overburden and plate tectonic causes and the horizontal x axis, through the relation

$$\tan 2\theta_R = 2\tau_{xyc}/(\sigma_{xc} + \sigma_{xP} - \sigma_{yc}). \tag{4}$$

3. Results

3.1 *Stresses due to combined effects of topography, buoyancy and crustal overburden*

Figure 3 displays the variation of σ_{xc}, σ_{yc} and τ_{xyc} due to the combined effects of topography, buoyancy and crustal overburden. The vertical normal stress, σ_{yc}, is

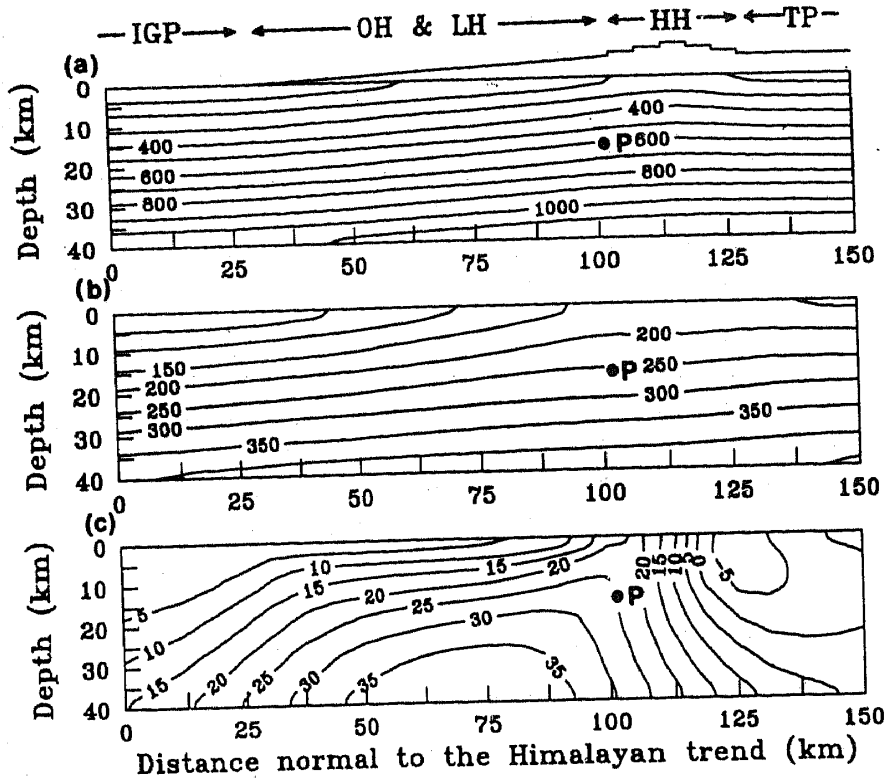

Figure 3. Contours of normal stress σ_{yc} (part a) and σ_{xc} (part b) as well as shear stress τ_{xyc} (part c) due to the combined effect of Himalayan topography, buoyancy and crustal overburden. Values of stresses are in MPa. Positive values of shear stress (in part c) at a point implies tendency to produce southward motion of rocks above the horizontal plane through that point. Only one contour of negative τ_{xyc} appears in the upper right corner of figure 3(c).

dominant throughout the region examined in figure 3a. It has a relatively smooth variation and its magnitude increases with depth. The horizontal normal stress, σ_{xc}, has a similarly smooth variation (figure 3b). But the variation of shear stress, τ_{xyc}, is more complicated. For most points shown in figure 3c, it has a tendency to cause southward movement of rocks above the respective horizontal planes. However, at shallow depths under the northern part of the Higher Himalaya and Tibet the opposite sense of shear motion is revealed by our calculations. The magnitude of this stress does not exceed 30MPa in the upper crust. A consideration of the data plotted in figures 2a, b and c reveals that the corresponding maximum and minimum principal stresses are subvertical and subhorizontal respectively at all points considered.

Our calculations are based on the assumption that the overburden and plate tectonics stresses are vertical and horizontal exactly. Even for topography and buoyancy, the vertical normal stresses are dominant over the corresponding horizontal stresses. The shear stresses due to topography and buoyancy effects considered individually are counteracting. However, for points at shallow depths in the crust, shear stress due to topography is relatively larger in magnitude than that due to buoyancy. Hence the former controls the sense of shear slip on planes at shallow depths in the Himalayan crust.

3.2 *Plate tectonic stress for reactivation of a subhorizontal thrust fault at point P at a depth of 17 km below MSL under the MCT*

We have selected to discuss in detail the plate tectonic stress required for reactivation of a subhorizontal thrust fault at a point, called P in the sequel for specificness and brevity (see figures 2 and 3), at a depth of 17 km below MSL under the MCT for two reasons. Firstly, Kelleher *et al* (1973) have argued that usually a great thrust fault type earthquake at a convergent plate margin nucleates near the deepest point of rupture in the respective causative fault. Thus based on simulations for the causative rupture of the great Kangra earthquake of 1905 (Chander 1989; Gahalaut and Chander 1992 and Gahalaut *et al* 1994), we may tentatively assume that the deepest point of rupture for a great Himalayan earthquake is at a depth of about 17 km below MSL in the Himalaya. For the usual estimates of the dip of the detachment this depth should be attained in the vicinity of the MCT. Secondly, as argued by Ni and Barazangi (1984) many moderate Himalayan earthquakes also occur on the detachment near the MCT. σ_{xc}, σ_{yc} and τ_{xyc} have values of 262, 622 and 26 MPa respectively at the point P in our model.

It transpires from equation 1 that the corresponding σ_{xP} at P is a function of pore pressure. friction coefficient and dip of the detachment. Figure 4a is a display of contours of σ_{xP} as a function of pore pressure and frictional coefficient so that a subhorizontal thrust fault at P would be reactivated. It is observed that the magnitude of σ_{xP} decreases with increase in pore pressure and decrease in friction coefficient. In

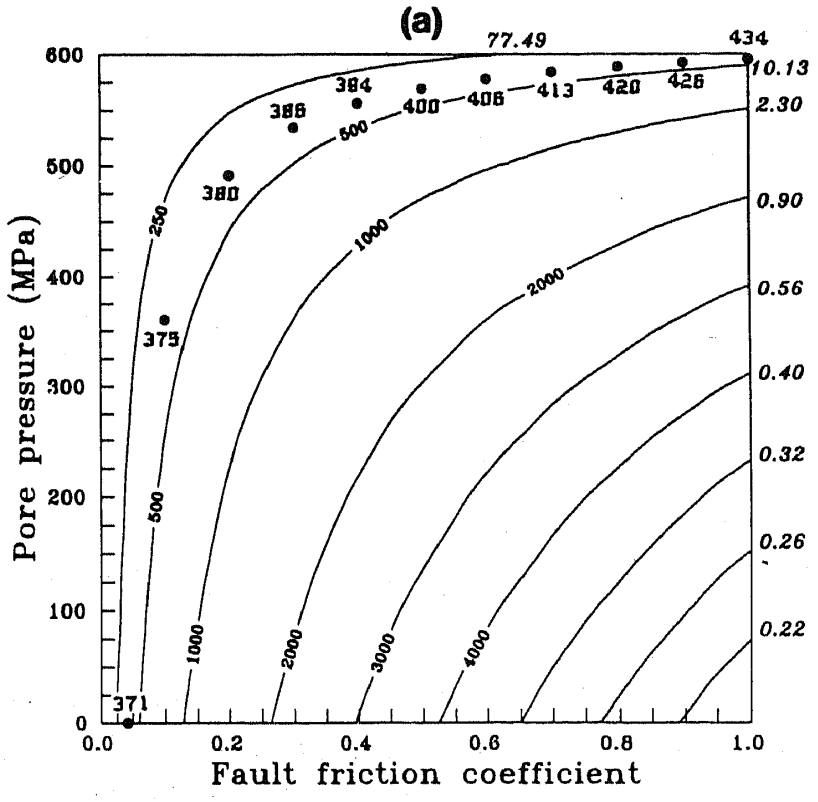

Figure 4a. (*Continued*)

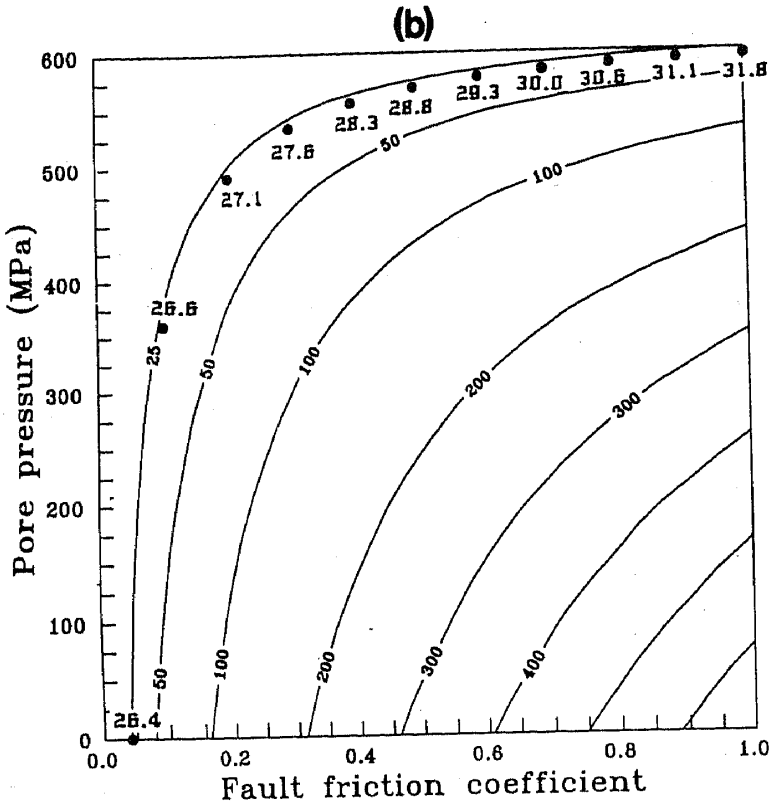

Figures 4a & b. Both figure 4(a) and (b) display results of calculations for point P on the detachment (see figure 2 and 3). Figure 4(a) shows contours of plate tectonic stress σ_{xP} as a function of pore pressure and fault friction coefficient. This stress when superimposed on those shown for P in figure 3(a), (b) and (c) would lead to reactivation of a subhorizontal thrust fault through P. Contour values are in MPa. Angle θ_R in degrees relevant to each contour is shown against it outside the figure at right and top. The dots identify values of σ_{xP} in MPa for favourably oriented resultant principal stresses (see section 3·3). There could be contours for even these values of σ_{xP} but they are omitted to avoid congestion. Figure 4(b) is similar to figure 4(a) except that it displays contours of total shear stress τ_F mobilized on a subhorizontal thrust fault at P for various values of σ_{xP} shown in figure 4(a).

view of equation 4, each contour of σ_{xP} in figure 4a is associated with a specific value of θ_R noted at the margin. σ_{xP} is in the range of 68 to 7947 MPa for friction coefficients in the range of 0 to 1·0 and zero pore pressure.

Another important parameter of interest is the total shear stress (τ_F, equation 2) mobilized on the subhorizontal thrust fault at P by the combined application of σ_{xP} and the stresses due to topography, buoyancy and overburden. Contours of τ_F as a function of pore pressure and friction coefficient are shown in figure 4b. τ_F has values in the range of 0 to 684 MPa for friction coefficient varying between 0 and 1·0 when the fault zone is in the dry state.

3.3 *Principal stresses oriented favourably for reactivation of subhorizontal faults*

3.3.1 *Range of* σ_{xP}: According to the Coulomb-Mohr theory, principal stresses at a point in a rock mass are oriented favourably for frictional failure on a pre-existing fault through that point when the maximum principal stress and the direction of

resolved shear stress in the fault plane is $45° - \phi/2$. In the present context, the maximum principal stress σ_{1R} will be oriented favourably for reactivation of the subhorizontal thrust faults when θ_R satisfies the following relation in addition to equation 4.

$$\theta_R = 45° - \phi/2 - \delta. \tag{5}$$

As mentioned above we have adopted a value of 5° for δ. θ_R then has a range of 40° to 17·5° for friction coefficient varying between 0 to 1·0. The corresponding range of σ_{xP} is only 369 to 434 MPa. Although we do not attempt identification of specific cause (s) of this plate tectonic stress, it is comforting to note that this magnitude for σ_{xP} is well within the range of the estimates for stresses from various specific plate tectonics related causes described by Bott and Kusznir (1984) (see discussion below).

3.3.2 *Range of* τ_F : Shear stress, τ_F, mobilized on the subhorizontal thrust fault at P by favourably oriented cumulative principal stresses varies between 26 and 32 MPa as the friction coefficient ranges between 0 to 1·0. These estimates of shear stress are in close agreement with the values of 20–30 MPa obtained by Bird (1978) for Himalayan faults currently. However, England and Molnar's (1993) estimate of shear stress on Himalayan intracrustal faults is of the order of 100 MPa on the assumption that frictional heating on faults was involved in the formation of Himalayan leuco- granites ca 18–20 Ma. Sibson (1986) estimated shear stresses of 10 to 100 MPa on crustal faults worldwide.

3.3.3 *Range of pore pressure*: The pore pressure required for reactivation of a subhorizontal fault at P under favourably oriented principal stresses is 0 for values of friction coefficient between 0 and 0·042. The pore pressure required increases rapidly for higher friction coefficient, attaining a value of 535 MPa for $\tan\phi = 0{\cdot}3$ (figure 4). But for still higher values of friction coefficient, the magnitude of required pore pressure increases more gradually to a value of 595 MPa for $\tan\phi = 1{\cdot}0$ (figure 4).

It is customary in diverse areas of earth sciences since the work of Hubbert and Rubey (1959) to compare crustal pore pressures with the lithostatic overburden stress. We have used above the term crustal overburden in the sense of material between MSL and the crustal depth of interest. However, we feel that the rock material in the Himalaya above MSL should also be taken into consideration for estimating lithostatic stress for such a comparison of pore pressure. The total magnitude of lithostatic overburden stress in 603 MPa for the point P. Thus we see that for all values of friction coefficient between 0 and 1·0, the pore pressure required for reactivation of a subhorizontal thrust fault at P is sublithostatic. We may recall that Davis *et al* (1983) also estimated a relatively high pore pressure of 0·76 lithostatic (or 458 MPa at P) for the Himalayan wedge using an entirely different approach.

3.3.4 *Narrow ranges of stresses and pore pressures*: A remarkable result of the preceding calculations is that σ_{xP} and τ_F at P have relatively narrow ranges between 371 to 434 MPa and 26 to 32 MPa respectively for friction coefficient varying between 0·04 to 1·0 (figure 4) when principal stresses are oriented favourably for fault reactiva- tion. Similarly, if very low friction coefficient (less than 0·3) on the Himalayan thrust faults are ruled out then the pore pressures required too have a narrow range between 535 to 595 MPa (figure 4). The ranges of these estimated values are so narrow, that their respective means may be taken as reference values in the upper crust under the Outer

and Lesser Himalaya. Alternatively, for reference purposes, we may use the values of these quantities corresponding to the nominal value of 0·65 for fault friction coefficient (Zoback 1992). These values are 409 MPa, 30 MPa and 581 MPa for σ_{xP}, τ_F and pore pressure respectively. These values are quoted in the abstract and conclusion as 410, 30 and 580 MPa after rounding off.

3.4 *Stresses for the reactivation of detachment under the Outer and Lesser Himalaya*

Since the current view about the ruptures of great Himalayan earthquakes is that they extend in the detachment updip from the vicinity of MCT at the deepest point to the vicinity of the MFT at the southern limit of the outer Himalaya, we have tried to estimate the stresses for reactivation of the detachment at various levels in this range.

Figure 5 is a display of the variation of σ_{xP}, τ_F and pore pressure required for reactivation of the detachment assuming most favourably oriented principal stresses and a nominal friction coefficient of 0·65. The range of variation of σ_{xP} over this stretch of the detachment is 409 to 100 MPa. The shear stress, τ_F, for reactivation of the detachment has a range of 30 to 7 MPa. Finally, the pore pressures vary correspondingly between 581 to 160 MPa.

3.5 *Stresses for reactivation of subhorizontal thrust faults at different depths beneath the MCT*

Since thrust fault type moderate Himalayan earthquakes are reported to have focal depths of 10 to 18 km (Ni and Barazangi 1984; Molnar 1990 and Zhao and Helmberger 1991), we have estimated the σ_{xP}, τ_F and pore pressure required for reactivation of subhorizontal thrust faults at various depths in this range. Since the Himalayan seismic belt defined by epicentres of moderate Himalayan earthquakes lies in the Lesser Himalaya close to the MCT, we have done the calculations for various crustal depths beneath the MCT for the sake of specificness. This set of calculations is-motivated also by the fact that the moderate 1991 Uttarkashi earthquake has been assigned a depth of 10 km by USGS using depth phases and its epicentre was in the MCT region in the Garhwal Himalaya. Again all the results quoted are for friction

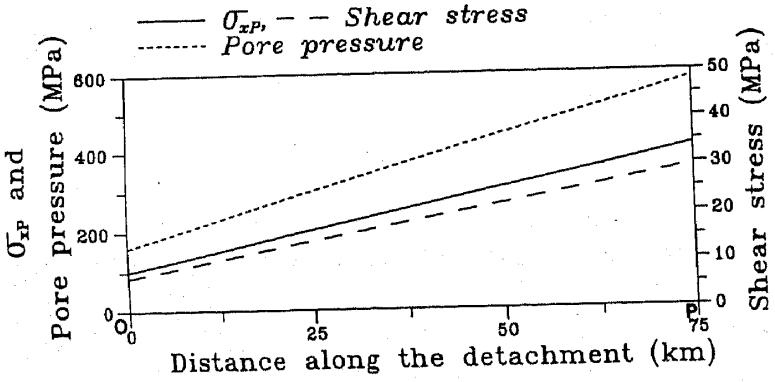

Figure 5. Variation of σ_{xP}, shear stress (τ_F) and pore pressure required for reactivation of the detachment between points *O* and *P* of figure 2. It is assumed that resultant principal stresses are favourably oriented for fault reactivation.

coefficient of 0·65 on the subhorizontal thrust faults and favourable orientation of principal stresses. σ_{xP} has a range of 409 to 54 MPa for a depth range of 17 to 1 km below MSL (figure 6). The shear stress required to be mobilized on the faults varies between 30 and 27 MPa only and required pore pressures vary between 581 to 124 MPa correspondingly (figure 6).

4. Discussion

4.1 *Method of analysis*

The preceding calculations are based on a relatively simplified evaluation of stresses due to various causes. However, there is fair agreement between our estimates of shear stresses and pore pressures required for reactivation of subhorizontal thrust faults in the Himalaya with those reported in the literature using different approaches. We discuss below the reasonableness of our simulation for the plate tectonic stress field. This provides strong support and justification for our method and calculations.

4.1.1 *Estimation of stresses due to crustal overburden*: An anonymous referee has inquired about the consequences of assuming a hydrostatic state for estimating stresses due to crustal overburden. He has referred to an article by McGarr (1988) where the latter has argued that the state of lithospheric stress in the absence of applied tectonic forces should be hydrostatic. At a cursory level as far as the present calculations are

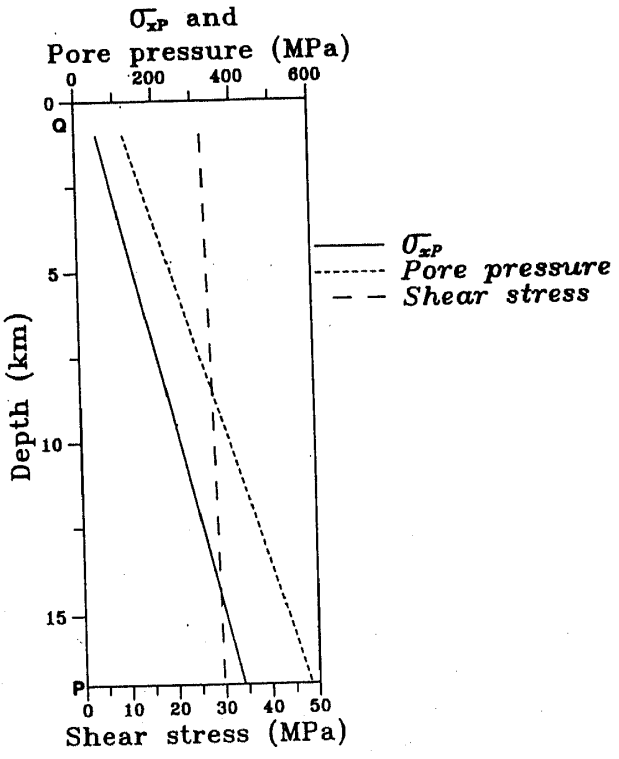

Figure 6. Similar to figure 4 showing variations of the same quantities for points between *P* and *Q* of figure 2.

concerned the most obvious difference would be that the estimates of plate tectonic stresses would be reduced by 2/3 of the vertical stress due to overburden. At a deeper level this is a fundamental, philosophical question requiring considerable further debate and investigations. Still we recall the opposing statement by Jeffreys (1962) that there must be stress differences in the earth. Since our interest here is in the simulation of earthquake generating stresses which are of more or less short time duration, depending upon the return period of earthquakes, therefore the calculations based on the elastic stress model assumed by us in section 2·3 should provide reasonable first estimates. But we shall look into it further.

4.2 *Relative magnitudes of normal and shear stresses*

A significant feature of the above calculations is that normal stresses are relatively high in comparison with shear stresses at all points in the crustal model of Himalaya visualized by us. This holds especially when the principal stresses are assumed to be oriented favourably for fault reactivation. The values of σ_F and τ_F are 627 MPa and 30 MPa for a friction coefficient of 0·65. Thus it is not surprising that a relatively high pore pressure of 581 MPa has to be postulated for reactivation of subhorizontal thrust faults.

4.3 *Causes of plate tectonic stress*

Bott and Kusznir (1984) list a number of factors which could give rise to stresses in a lithospheric plate under different circumstances. Ridge push, asthenosphere shear drag and plate bending due to subduction appear suitable for the Himalaya at first sight. But the first two factors may give rise to stresses only upto 50 MPa each, while the third factor could lead to stresses upto 1000 MPa (Bott and Kusznir 1984). Ridge push gives rise to compressive stresses only, but the stresses due to shear drag and plate bending could be compressive as well as tensile. Thus, contributions to σ_{xP} from ridge push and shear drag could be involved certainly. But plate bending stresses due to subduction requires comment. Since σ_{xP} at P is compressive and has a magnitude which is nearly 40% of the maximum estimated stress from this cause (Bott and Kusznir 1984), P would have to be reasonably below the neutral surface of a plate flexed convex upward. This in turn implies that either the bent plate in the Himalaya is relatively thin or the Himalayan rocks above the detachment are decoupled from the underthrusting Indian shield material and thus flex independently as a plate. But since σ_{xP} according to our calculation is compressive throughout the Himalayan upper crust, it is unlikely that such plate bending could be the exclusive cause of the computed σ_{xP} field because we have to anticipate tensile stresses above the neutral surface. Although not considered specifically by Bott and Kusznir (1984), a possibility to meet this objection could be that Himalayan upper crustal rocks could be flexed convex downward on a regional scale. But an objection to this idea arises because the magnitude of σ_{xP} decreases upward according to our calculations whereas stresses due to such plate bending would increase upward in the model. Still another possibility worth considering is that the upper crustal rocks in the Himalaya may experience large horizontally oriented compressive stresses as a result of continent- continent collision that leads to crustal thickening.

Thus while identification of a specific set of plate tectonic causes for the estimated field of σ_{xP} under the Himalaya is a topic for further investigations, there is no doubt that the magnitudes of σ_{xP} estimated by us are well within the realm of possibility keeping in mind Bott and Kusznir's (1984) estimates of stresses that can be mobilized from different plate tectonic causes.

4.4 *Reduction in normal stress on the fault*

Referee J Brune has drawn our attention to the very exciting idea that at the time of nucleation of an earthquake, the normal stress on the fault may be reduced by causes other than pore pressure, vibrations being one of them. Brune *et al* (1990), Brune *et al* (1993) and Anooshehpoor and Brune (1994) report experiments with foam rubber models which give credence to this concept. They also support the argument by citing theoretical reasoning of Haskell (1964) and observations from a seismic array in southern California for anomalous P wave excitation which might be produced by normal vibrations of the fault interface at the time of earthquake nucleation. Brune *et al* (1993) and Anooshehpoor and Brune (1994) have applied this concept to the so called heat flow paradox along the San Andreas fault. The idea deserves scrutiny in the Himalayan context also. Observational evidence in the form of anomalous P wave radiation from Himalayan earthquakes would require installation of digital seismograph arrays in the Himalaya. The irony of the situation is that there seems to be an effort in some official and civil engineering circles to deemphasize observational seismology in India generally and the Himalaya parti- cularly (Midha 1994 and Chander 1995).

5. Conclusions

- We may conclude, inspite of the various assumptions and the simplified analytical approach adopted for simulating earthquake generating stresses in the Himalayan upper crust, that our estimates for plate tectonic stresses are within the realm of possibility while estimates of shear stresses and pore pressures are comparable to those reported in the literature.
- If it is assumed that the cumulative principal stresses are favourably oriented for earthquake related reactivation of a subhorizontal thrust fault having a nominal friction coefficient of 0·65 and located at a point 17 km beneath MSL under the MCT, then σ_{xP}, τ_F and pore pressure should have values of about 410 MPa, 30 MPa and 580 MPa respectively.
- According to our calculations, nearly uniform, but sublithostatic, pore pressures can lead to failure for a relatively wide range of 0·3 to 1·0 for friction coefficient on the subhorizontal thrust faults. Hence we conclude that unreasonably low values of fault friction coefficient need not be invoked but the presence of water in the intra- crustal fault zones of the Himalaya is essential for the occurrence of great and moderate earthquakes.

Acknowledgement

Financial support of UGC to VKG is acknowledged.

Appendix

We compute the stress field under the Himalaya considering two-dimensional plane strain theory. The x axis is assumed horizontal and directed northerly perpendicular to the local trend of the arcuate Himalaya. The y axis is vertical and pointing downward.

The various symbols used in the text are explained in the following table.

ϕ	: angle of friction and $\tan\phi$ is the coefficient of friction.
$\sigma_{xc}, \sigma_{yc}, \tau_{xyc}$	: normal and shear stresses on planes perpendicular to x and y axis due to combined effect of topography, buoyancy and overburden load.
σ_{xP}	: Horizontally directed compressive normal stress of plate tectonic origin.
σ_{1R}, σ_{3R}	: maximum and minimum principal stresses due to the combined effect of topography, buoyancy, overburden and plate tectonic causes.
σ_F, τ_F	: resultant normal and shear stresses on the detachment.
p	: pore pressure.
δ	: dip of the detachment.
θ_R	: the direction of σ_{1R} from the x axis, considered positive upward.

The sign convention adopted for stresses is that compressive normal stresses are assumed positive. Similarly shear stresses promoting reactivation of thrust faults in the Himalaya are considered positive.

References

Anooshehpoor A and Brune J N 1994 Frictional heat generation and seismic radiation in a foam rubber model of earthquakes; *PAGEOPH* **142** 735–747

Baranowski J, Armbruster J, Seeber L and Molnar P 1984 Focal depths and fault plane solutions of earthquakes and active tectonics of the Himalaya; *J. Geophys. Res.* **89** 6918–6928

Bird P 1978 Initiation of intracontinental subduction in the Himalaya; *J. Geophys. Res.* **83** 4975–4987

Bott M H P and Kusznir N J 1984 The origin of tectonic stress in the lithosphere; *Tectonophysics* **105** 1–13

Brune, J N, Brown S and Johnson P A 1993 Rupture mechanism and interface separation in foam rubber models of earthquakes: a possible solution to the heat flow paradox of large overthrusts; *Tectonophysics* **218** 59–67

Brune J N, Johnson, P A and Slater C 1990 Nucleation, predictability and rupture mechanism in foam rubber models of earthquakes; *J. Him. Geol.* **1** 155–166

Burchfiel B and Royden L H 1985 North-South extension within the convergent Himalayan region; *Geology* **13** 679–682

Chander R 1988 Interpretation of observed ground level changes due to the 1905 Kangra earthquake, Northwest Himalaya; *Tectonophysics* **149** 289–298

Chander R 1989 Southern limits of major earthquakes ruptures along the Himalaya between longitudes 75° and 90°E; *Tectonophysics* **170** 115–123

Chander R 1995 On the need to install seismographs in the Himalayas; *Curr. Sci.* **68** 239

Davis D, Suppe J and Dahlen F A 1983 Mechanics of fold-and-thrust and accretionary wedges; *J. Geophys. Res.* **88** 1153–1172

England P and Molnar P 1993 The interpretation of inverted metamorphic isograds using simple physical calculations; *Tectonics* **12** 145–157

Fitch T J 1970 Earthquake mechanisms in the Himalayan, Burmese and Andaman regions and the continental tectonics in central Asia; *J. Geophys. Res.* **75** 2699–2709

Forsyth D and Uyeda S 1975 On the relative importance of the driving forces of plate motion; *Geophys. J. R. Astron. Soc.* **43** 163–200

Gahalaut V K and Chander R 1992 On the active tectonics of Dehradun region from observations of ground level changes; *J. Geol. Soc. India* **39** 61–68

Gahalaut V K, Gupta P K, Chander R and Gaur V K 1994 Minimum norm inversion of observed ground elevation changes for slips on the causative fault during the 1905 Kangra earthquake; *Proc. Indian Acad. Sci. (Earth Planet. Sci.)* **103** 401–411

Gansser A 1964 *Geology of the Himalayas* (London: Intersci. publ. John Wiley) pp. 289

Haskell N 1964 Total energy and energy spectral density of elastic wave radiation from propagating fault; *Bull. Seismol. Soc. Am.* **54** 1811–1841

Hubbert M K and Rubey W W 1959 Role of fluid pressures in mechanics of overthrust faulting: 1. Mechanics of fluid filled porous solids and its application to overthrust faulting; *Bull. Geol. Soc. Am.* **70** 115–166

Jeffreys H 1962 *The Earth* (Cambridge Univ. Press) pp. 438

Jaeger J C and Cook N 1969 *Fundamentals of rock mechanics* (London: Methuen) pp. 513

Karner G D and Watts A B 1983 Gravity anomalies and flexure of the lithosphere at mountain ranges; *J. Geophys. Res.* **88** 10449–10477

Kelleher J A, Sykes L R and Oliver J 1973 Possible criteria for predicting earthquake locations and their applications to major plate boundaries of the Pacific and Caribbean; *J. Geophys. Res.* **78** 2547–2585

Lyon-Caen H and Molnar P 1985 Gravity anomalies, flexure of the Indian plate and structure, support and evolution of the Himalaya and Ganga basin; *Tectonics* **4** 513–538

McGarr A 1988 On the state of lithospheric stress in the absence of applied tectonic forces; *J. Geophys. Res.* **93** 13609–13617

Midha R K 1994 Latur earthquake: some major initiatives by DST; *Deep continental studies in India, Newsletter for deep continental studies,* (ed) B R Arora (Bombay: Indian Institute of Geomagnetism) **4** 8–10

Molnar P 1990 A review of the seismicity and the rates of active underthrusting and deformation at the Himalaya; *J. Himalayan Geol.* **1** 131–154

Ni J and Barazangi M 1984 Seismotectonics of the Himalayan Collision zone: Geometry of the underthrusting Indian plate beneath the Himalaya; *J. Geophys. Res.* **89** 1147–1163

Seeber L and Armbruster J 1981 Great detachment earthquakes along the Himalayan arc and long-term forecasting; In *Earthquake prediction. An international review* Maurice Ewing series 4 (eds) D W Simpson and P G Richards (Washington D C: Am. Geophys. Union). pp. 259–277

Sibson R H 1986 Earthquakes and rock deformation in crustal fault zones; *Annu. Rev. Earth Planet. Sci.* **14** 149–175

Yeats R S and Lillie R J 1991 Contemporary tectonics of the Himalayan frontal fault system: folds, blind thrusts and the 1905 Kangra earthquake; *J. Struct. Geol.* **13** 215–225

Zhao L S and Helmberger D V 1991 Geophysical implications from relocations of Tibetan earthquakes; Hot lithosphere; *Geophys. Res. Lett.* **18** 2205–2208

Zhao W, Nelson K D and Project INDEPTH team 1993 Deep seismic reflection evidence for continental underthrusting beneath southern Tibet; *Nature* (London) **366** 557–559

Zoback M L 1992 First-and Second-order patterns of stress in the lithosphere: The world stress map project; *J. Geophys. Res.* **97** 11703–11728